

We are IntechOpen, the world's leading publisher of Open Access books Built by scientists, for scientists

6,900

Open access books available

186,000

International authors and editors

200M

Downloads

Our authors are among the

154

Countries delivered to

TOP 1%

most cited scientists

12.2%

Contributors from top 500 universities



WEB OF SCIENCE™

Selection of our books indexed in the Book Citation Index
in Web of Science™ Core Collection (BKCI)

Interested in publishing with us?
Contact book.department@intechopen.com

Numbers displayed above are based on latest data collected.
For more information visit www.intechopen.com



Heat Transfer in Freeze-Drying Apparatus

Roberto Pisano, Davide Fissore and Antonello A. Barresi
Dipartimento di Scienza dei Materiali e Ingegneria Chimica, Politecnico di Torino
Italy

1. Introduction

Freeze-drying is a process used to remove water (or another solvent) from a frozen product, thus increasing its shelf-life. It is extensively used in pharmaceuticals manufacturing, to recover the active pharmaceutical ingredient (and the excipients) from an aqueous solution, as well as in some food processes, because of the low operating temperatures that allow preserving product quality. Moreover, the freeze-dried product has a high surface area and can be easily re-hydrated.

In this chapter we focus on pharmaceuticals manufacturing, where the solution containing the product is generally processed in vials, placed over the shelves in a drying chamber. However, it is worth stating that, in industrial practice, other loading configurations can be used to carry out the process, thus this study will be extended also to the case where vials are loaded on trays, or the solution is directly poured in trays. The process consists of three consecutive steps, namely:

1. Freezing: product temperature is lowered below the freezing point and, thus, most of the solvent freezes, forming ice crystals. Part of the solvent can remain bounded to the product, and must be desorbed. Also the product often forms an amorphous glass which can retain a high amount of water.
2. Primary drying: in this step the pressure in the drying chamber is lowered, thus causing ice sublimation. This phase is usually carried out at low temperature (ranging, in most cases, from -40°C to -10°C) and, as sublimation requires energy, heat is transferred to the product through the shelf, by acting on the temperature of the fluid flowing in the coil inserted in the shelf.
3. Secondary drying: when the sublimation of the ice has been completed, shelf temperature is raised (e.g. to $20-40^{\circ}\text{C}$) and chamber pressure is further decreased to allow the desorption of the water bounded to the product, thus getting the target moisture in the product.

The freeze-dryer comprises the drying chamber and a condenser where the water vapour is sublimated on some cold surfaces in order to decrease the volumetric flow-rate arriving to the vacuum pump. The pressure in the chamber can be modified either by acting on a valve placed on pump discharge, or using the so called “controlled leakage”, i.e. manipulating the flow rate of nitrogen (or another gas) introduced in the chamber. The drying chamber can be isolated from the condenser by means of a valve that is usually placed in the duct connecting the chamber to the condenser (Mellor, 1978; Jennings, 1999; Oetjen & Haseley, 2004; Franks, 2007).

Although it is generally considered a “soft” drying process, because of the low operating temperatures, the heat transfer to the product has to be carefully controlled in order to avoid product overheating. In fact, product temperature has to be maintained below a limit value to avoid the occurrence of undesired events. In case of products that crystallize during freezing, the limit temperature corresponds to the eutectic point: the goal is to avoid the formation of a liquid phase and the successive boiling due to the low pressure. In case the product remains amorphous during freezing, the maximum allowed product temperature is close to the glass transition temperature in order to avoid the collapse of the dried cake: this value can be very low, and is also dependent on the residual moisture. The occurrence of collapse can increase the residual water content in the final product and the reconstitution time, beside decreasing the activity of the pharmaceutical principle; moreover, a collapsed product is often rejected because of the unattractive physical appearance (Pikal & Shah, 1990; Wang, 2000; Rambhatla et al., 2005; Sadikoglu et al., 2006). Beside product temperature, also the residual amount of ice in the product has to be carefully controlled during primary drying, thus identifying the ending point of this phase. In fact, if shelf temperature is increased too early to the value required by the last phase of the cycle, product temperature may exceed the maximum allowed value, thus causing melting or collapse. Also in this case heat transfer to the product plays a key role as, at steady-state, the following equation holds:

$$J_q = \Delta H_s J_w \quad (1)$$

where J_q is the heat flux to the product, J_w is the solvent flux from the product to the chamber, and ΔH_s is the heat of sublimation.

In this chapter, thus, we will focus on heat transfer in vial, as well as bulk, freeze-drying as it is one of the key factor affecting product dynamics and temperature. In particular, the results previously presented by Pikal (2000) for vial freeze-drying are here extended.

The techniques allowing to calculate the heat transfer parameters, or to estimate their values by means of experiments, will be briefly reviewed. We will point out that the heat flux between the heating shelf and the container is the result of several mechanisms that depend on dryer and container geometry, as well as on pressure and temperature of the surrounding gas. Moreover the heat flux to the batch of vials is far from being uniform in a freeze-dryer: the implications on recipe design and scale-up will be finally addressed.

2. Theoretical calculation of heat flux in vial freeze-drying

The heat flux to the product is proportional to the difference between the heating fluid temperature (T_{fluid}) and the product temperature at the vial bottom (T_B):

$$J_q = K_v (T_{\text{fluid}} - T_B) \quad (2)$$

where K_v is the heat transfer coefficient. It has to be highlighted that in eq. (2) it has been assumed that product temperature is uniform in the radial direction, as it has been demonstrated by means of mathematical simulation and experimental investigations (Pikal, 1985; Sheehan & Liapis, 1998).

Various equations can be found in the literature to calculate the heat exchange coefficient K_v in case the vial is placed directly over the shelf, i.e. if no tray is used. These relationships are still valid in case the solution is directly poured in a tray.

Firstly, the heat transfer coefficient between the heating shelf and the bottom of the vial (K_v') is calculated as the sum of three terms:

$$K_v' = K_c + K_r + K_g \quad (3)$$

corresponding to the various heat transfer mechanisms between the fluid and the vial bottom, namely the direct conduction from the shelf to the glass at the points of contact (K_c), the radiation (K_r), and the conduction through the gas (K_g). In this study, we assume that all these contributions can be referred to the same heat transfer area.

According to Smoluchowski theory, as outlined by Dushman & Lafferty (1962) and reported by Pikal et al. (1984), K_g is a function of the average distance between the bottom of the vial and the shelf (ℓ) and of chamber pressure:

$$K_g = \frac{\alpha \lambda_0 P_c}{1 + \ell \left(\frac{\alpha \lambda_0}{\lambda_0} \right) P_c} \quad (4)$$

The parameter α is a function of the energy accommodation coefficient and of the absolute temperature of the gas:

$$\alpha = \frac{a_c}{2 - a_c} \cdot \sqrt{\frac{273.2}{T}} \quad (5)$$

When other gases, beside water vapour, are present in the drying chamber (e.g. nitrogen entering the chamber when controlled leakage is used to regulate the pressure), eqs. (4) and (5) have to be modified to take into account gas composition, as total pressure is due to the sum of the contribution of water and nitrogen partial pressures (Brülls & Rasmuson, 2002). It has to be remarked that the bottom of the vial is not flat, and the curvature depends on the type of vial: thus, the value of K_g is a function of the type of vial considered.

Beside conduction in the gas, there are two radiative heat fluxes towards the product, one from the shelf upon which the vials rest, and the other from the top. Each flux is proportional to the difference in the fourth powers of the absolute temperatures of the two surfaces, and to the effective emissivity for the heat exchange, which depends on the relative areas of the two surfaces, their emissivities, and a geometrical view factor. According to Pikal et al. (1984) the radiative heat transfer coefficient can be written as:

$$K_r = 4(e_s + e_v) \kappa T^3 \quad (6)$$

While the values of λ_0 , λ_0 , and e_s can be found in the literature, the values of the parameters K_c , a_c , ℓ , and e_v (in case radiation from upper shelf plays an important role), have to be determined by regression analysis of experimental data, even if some values can be found in the literature for some types of vials (Pikal et al., 1984).

It follows that K_v' depends essentially on the operating conditions at which drying is carried out: chamber pressure, shelf temperature and, in turn, temperature of chamber gas. However, according to literature (Hottot et al., 2005) and to the results shown in the following, the dependence of K_v' on chamber gas temperature is not relevant. On the contrary, the heat transfer between the shelf and the container significantly varies with chamber pressure, and this dependence can be well described by a nonlinear equation with the following structure:

$$K'_v = C_1 + \frac{C_2 \cdot P_c}{1 + C_3 \cdot P_c} \quad (7)$$

where:

$$\begin{cases} C_1 = K_c + 4\kappa \bar{T}^3 (e_s + e_v) \\ C_2 = \frac{a_c}{2 - a_c} \sqrt{\frac{273.2}{T}} \Lambda_0 \\ C_3 = \ell \left(\frac{\Lambda_0}{\lambda_0} \frac{a_c}{2 - a_c} \sqrt{\frac{273.2}{T}} \right) \end{cases} \quad (8)$$

At this point, K'_v can be calculated, whichever are the processing conditions, provided that a_c , K_c and ℓ (and thus C_1 , C_2 and C_3) are known.

If vials are loaded on a tray, the shelf-vial system can be described as a set of resistors in series, whose total resistance is the sum of their individual resistances. It follows that the resistance for the mentioned system can be expressed as the sum of the resistance due to tray thickness, as well as to the shelf-tray and tray-vial heat transfers that can be both described by equations similar to eq. (7). Provided that the heat transfer between shelf and tray ($K'_{v,1}$), and from tray to vials ($K'_{v,2}$), can be described by the same equations, we can define K'_v as an effective heat transfer coefficient that accounts for both contributions:

$$\frac{1}{K'_v} = \frac{1}{K'_{v,1}} + \frac{1}{K'_{v,2}} \quad (9)$$

It is worth noticing that, as a consequence of this assumption, the value of the global coefficients of eq. (7) (i.e. C_1 , C_2 and C_3), as determined by a regression analysis of experimental observations, are effective values that take into account both the heat transfer between shelf and tray and tray and vials.

The coefficient K_v^* (from the shelf surface to product bottom) can be calculated by taking into account the conduction in the glass at the bottom of the vial, as well as through the tray (if it is used):

$$K_v^* = \frac{J_q}{T_{\text{shelf}} - T_B} = \left(\frac{1}{K'_v} + \frac{s_g}{\lambda_g} + \frac{s_{\text{tray}}}{\lambda_{\text{tray}}} \right)^{-1} \quad (10)$$

In addition, if the considered driving force for the heat transfer is the temperature difference between the heating fluid and the product, we have also to include the resistance to heat transfer through shelf ($1/k_s$). Therefore, eq. (10) has to be substituted by:

$$K_v = \left(\frac{1}{K'_v} + \frac{s_g}{\lambda_g} + \frac{s_{\text{tray}}}{\lambda_{\text{tray}}} + \frac{1}{k_s} \right)^{-1} \quad (11)$$

Finally, it has to be remarked that the product in the vial can receive heat from the walls of the container, as well as from chamber walls, due to radiation. Both contributions do not appear explicitly in eq. (2), but the coefficient K_v can be regarded as an effective heat transfer

coefficient, weighing up these additional heat fluxes (Velardi & Barresi, 2008). However, as it will be discussed in the following sections, it is worth remarking that the contribution of radiative heat to the total energy balance of the vial can vary with its position over the shelf. This phenomenon, together with the presence of fluid temperature gradients along the shelf, is responsible for lot unevenness.

3. Experimental methods for K_v measurement

Various methods have been proposed in the past to determine the value of the coefficient K_v (or that of K'_v). They are briefly reviewed in the following.

A very simple test that allows determining the coefficient K_v consists of preparing a batch of vials filled with the product, a placebo, or simply water and, then, to carry out the primary drying for a time interval (Δt) and to measure the weight loss (Δm) and the temperature of the ice at the vial bottom (T_B). The coefficient K_v is given by:

$$K_v = \frac{\Delta m \cdot \Delta H_s}{\Delta t \cdot (T_{\text{fluid}} - T_B) \cdot A_v} \quad (12)$$

As the heat transfer coefficient is a function of chamber pressure, at least three measurements at three different values of P_c are required to calculate the global coefficients of eq. (7).

During the drying, the temperature of the heating fluid can vary along the shelf as the heat is transferred from the technical fluid to the product. However, it must be said that generally the inlet-outlet fluid temperature difference observed under full-load conditions is small (typically lower than 1 K) and of the same order of magnitude of temperature sensor uncertainty. A similar behaviour has been observed in all the experiments whose results are reported in this chapter. It follows that it is not necessary to take into account explicitly the fluid temperature gradient along the shelf in the calculation of K_v , as its effect can be included in the uncertainty of the parameter.

On the other hands, the value of the coefficient K_v is not the same for all the vials of the lot, as a consequence of the different contributions of the various heat transfer mechanisms: as an example, the vials at the edges of the shelf receive also radiant heat from the chamber walls, while the vials located in the central part of the batch are heated only from the heating fluid (Pikal, 2000; Rambhatla & Pikal, 2003; Gan et al., 2005a, 2005b). As a consequence, a different evolution of product temperature can be observed in vials located in various positions of the batch. Therefore, to estimate accurately K_v for each class of vials, product temperature has to be monitored, and thus thermocouples must be inserted both in vials placed in the core and at the edge of the lot.

According to their position over the shelf, the vials of a lot can be classified in various groups depending on the different heat transfer mechanisms involved. In particular, in case vials are confined by a metal or plastic band, we can generally identify five zones (see Figure 1), which are characterized by different heat transfer mechanisms, as reported in Table 1.

A further refinement might be introduced to distinguish edge vials that are exposed to different walls of the drying chamber. This is particularly true for laboratory scale equipment, where the dryer door is not made of steel (like the other chamber walls), but of Plexiglas. Since the two materials have a significantly different value of emissivity (0.36 vs. 0.95), vials close to the door may show a higher value of K_v with respect to the rest of the lot

(Rambhatla & Pikal, 2003). On the contrary, in a manufacturing plant, the dryer door is usually made of steel and, thus, edge vials are less uneven. Nevertheless, it must be said that in a large scale equipment only a limited fraction of vials are radiated, while in a laboratory dryer (where the fraction of edge vials is much greater) the contribution of the radiative heat can be strongly reduced by a proper shielding. These differences, however, must be taken into account during scale-up of a recipe from laboratory to industrial scale dryers.

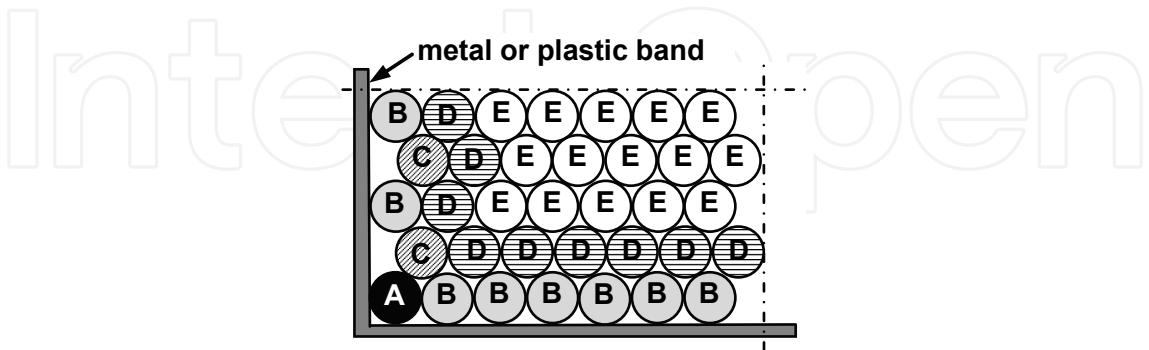


Fig. 1. Scheme of a lot, wherein vials have been classified depending on their position and on the additional heat transfer mechanisms involved

Vial group	Position over the shelf	Additional mechanisms to vial heat transfer		
		<i>radiation from chamber walls</i>	<i>contact with the tray band</i>	<i>contact with "hot" vials</i>
A	corner	yes	yes	yes
B	peripheral	yes	yes	yes
C	peripheral	yes	no	yes
D	core	no	no	yes
E	core	no	no	no

Table 1. Characteristics of the various vial families with respect to the position on the shelf and the mechanisms of heat transfer involved

It must be remarked that the gravimetric measurement is the only method that gives a detailed picture of single vial behaviour and of interval variability, thus allowing to identify the various vial families. A heat flux transducer can also be used for monitoring the dynamics of the single vials composing the lot (Chen et al., 2008), but its use implies that the monitored vials are loaded on the sensor surface altering de facto the heating conditions. Equation (12) can be still used when the sublimation flux (i.e. $\Delta m/\Delta t \cdot A_v$) is obtained by other means, for example using the Tunable Diode Laser Absorption Spectroscopy (TDLAS) or the pressure rise test technique.

The Doppler-shifted near-infrared absorption spectroscopy is used for measuring the water vapour concentration and gas flow velocity in the duct (that connects drying and condenser chamber). At this point, these variables can be used, known the cross-sectional area of the duct, to estimate the vapour flow rate (Kessler et al., 2006; Gieseler et al., 2007). It must be remarked that TDLAS does not measure directly the mass flow, but only the gas flow velocity in a limited number of points; therefore, the reliability of the vapour flow rate estimation depends on how well the velocity profile is known. This is a critical issue, since

the velocity profile continuously develops in the duct, tightly depends on processing conditions, can be strongly modified by the presence of Clean In Place systems, and even at the duct exit is usually far from the parabolic profile corresponding to fully developed flow. Other drawbacks of this technique are the high investment costs, the difficult to retrofit existing units, and the difficulties in its calibration.

To measure the vapour flow rate (and hence the heat transfer coefficient), an alternative solution, that can be easily implemented also in existing devices, is the pressure rise test technique: the valve in the duct connecting the drying chamber to the condenser is closed for a short time interval, and, thus, pressure in the chamber increases due to vapour accumulation. Once the pressure rise curve has been acquired, the vapour flow rate (J_w) can be calculated by simply evaluating its slope at the beginning of the test (Fissore et al., 2011a):

$$J_w = \frac{V_c M_w}{A_{sub} R T_c} \left. \frac{dp_{w,c}}{dt} \right|_{t=t_0} \quad (13)$$

This measure of J_w is reliable as it is based on the direct measurement of the effect of the sublimation flow, the pressure increase, described by a simple physical law. Unlike TDLAS, the pressure rise technique can be used in both laboratory and industrial scale dryers, provided that drying and ice condenser chamber are separated, without any modifications of existing units. Figure 2 shows an example of pressure rise curves measured (at various time during the primary drying phase) in a laboratory and in an industrial scale dryer. These results were obtained during the drying of a 5% by weight mannitol solution. As stated before, the vapour flow rate is related to the slope of the pressure profile, which, as expected, decreases as the drying proceeds.

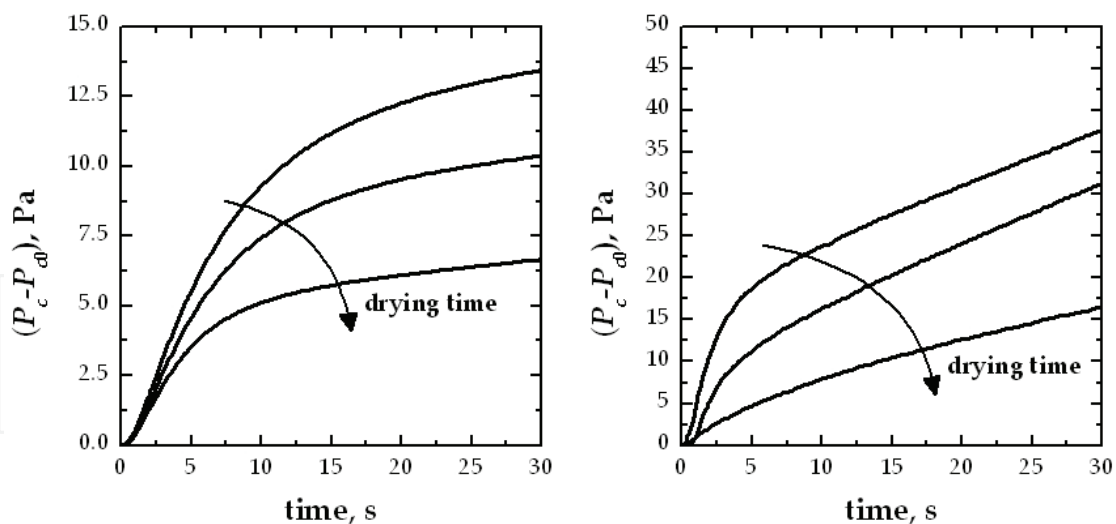


Fig. 2. Examples of pressure rise curves measured at various times during the primary drying stage in (left-side graph) a laboratory and (right-side graph) an industrial dryer

To calculate K_v from the vapour flow rate, the product temperature at the container bottom has to be measured, for example, inserting thermocouples in some vials. For this purpose, the use of wireless technology is promising (Corbellini et al., 2010; Schneid & Gieseler, 2008) as it is compatible with the restrictions of industrial equipment that typically uses automatic loading systems.

The pressure rise curve can be also described by a mathematical model, whose parameters (e.g. product temperature at the beginning of the test, and K_v) are retrieved by looking for the best fit between measured and calculated values of chamber pressure (Milton et al., 1997; Chouvinc et al., 2004; Tang et al., 2006; Velardi et al., 2008). The optimal selection of sampling frequency and duration of the test has been discussed by Fissore et al. (2011a), who also proposed a modification of the Dynamic Parameters Estimation algorithm (Velardi et al., 2008) to cope with the problem of ill-conditioning. It must be said that while the estimation of J_w from the slope of the pressure rise curve can be also carried out with pure ice, the previous algorithms (which take advantage of a model) require that a product, which gives a mass flow resistance, is used. In addition, unlike previous techniques, the pressure rise, coupled with one of the above cited algorithms, does not require an independent measurement of product temperature.

It is worth noticing that the gravimetric measurement is the only method that allows to determine the distribution of the values of K_v in the lot, while both the TDLAS sensor and the pressure rise test based methods allow to determine only a mean value of K_v for the batch. Nevertheless, it must be said that the fraction of edge-vials, and hence its contribution to the mean value of K_v , is becoming less and less important as the size of the dryer becomes larger.

In addition, it must be remarked that the above mentioned methods, differently from the gravimetric test, allow to get an estimation of K_v vs. P_c , even in only one run (Kuu et al., 2009; Pisano et al., 2010) if chamber pressure is properly varied during the test (e.g. as a multi-step constant function), without requiring an excessive effort from the users. Furthermore, these methods allow getting an estimation of K_v whichever is the scale of the equipment. In particular, this eases the problem of K_v measurement for industrial scale apparatus (as well as of process transfer) where the gravimetric procedure cannot be used since the intervention of the user is limited. Therefore, following on from what stated above, the use of global methods is strongly suggested for large scale apparatus.

4. Heat transfer in bulk and vials freeze-drying

In the following the influence of processing conditions, vial and tray characteristics and equipment size will be discussed in detail, presenting a selected set of original experiments planned by the authors to highlight the previous aspects.

In particular, experiments were carried out using both tubing vials (whose characteristics are reported in Table 2) and trays made of stainless steel or polystyrene. In case of freeze-drying in vials, it was also investigated the effect of various loading configurations (e.g. comparing the value of K_v for vials processed directly over the heating shelf or in trays), as well as of different pieces of equipment, not only on the mean value of K_v , but also on interval variability. With this respect, the gravimetric measurement is the only method that allows to get a complete description of the heat transfer in the lot. However, results obtained by the pressure rise test technique will be also presented, confirming the capacity of this method to get a quick and reliable estimation of the parameter of interest, not only in a laboratory equipment (*LyoBeta 25TM* by Telstar, Terrassa, Spain), but also in an industrial scale dryer where gravimetric experiments cannot be easily carried out. Previous results had already shown this, evidencing at the same time that inaccuracies of the PRT model can affect its reliability (Tang et al., 2006).

Properties	vials V ₁	vials V ₂	vials V ₃	vials V ₄
External diameter, mm	14.25	16.20	24.14	14.12
Thickness of side wall, mm	1.00	0.80	1.10	0.90
Thickness of vial bottom wall, mm	0.70	1.41	1.41	0.60
Estimated thickness of bottom vial gap (ℓ), mm	0.20	0.32	0.38	0.34

Table 2. Geometrical characteristics of the various glass vials investigated in this study

4.1 Influence of processing conditions on K_v

Figure 3 (left-side graph) displays the value of K_v vs. P_c measured by gravimetric way for a lot of vials (type V₁), which was directly loaded on the heating shelf and surrounded by a metal band. Vials placed in the central part of the shelf, i.e. those far from the edges where the effect of radiative heat coming from chamber walls can be relevant, are considered. According to Brülls & Rasmuson (2002) and Hottot et al. (2005), K_v increases with P_c , because of a higher heat conduction through the gas trapped between the tray and glass vial bottom.

In Figure 3 (left-side graph), it can be also observed a fairly good agreement between the value of K_v vs. P_c as measured by the pressure rise test technique (coupled with a modified version of Dynamic Parameters Estimation algorithm, DPE⁺) and by gravimetric way. The values of K_v vs. P_c predicted by the mathematical model described in section §2 is also displayed. The model parameters a_c , K_c and ℓ and, thus, the global coefficients C_1 , C_2 and C_3 (that describe the pressure dependence of K_v for vials V₁) were obtained by a non-linear regression of experimental data. The results so obtained are summarized in Table 3.

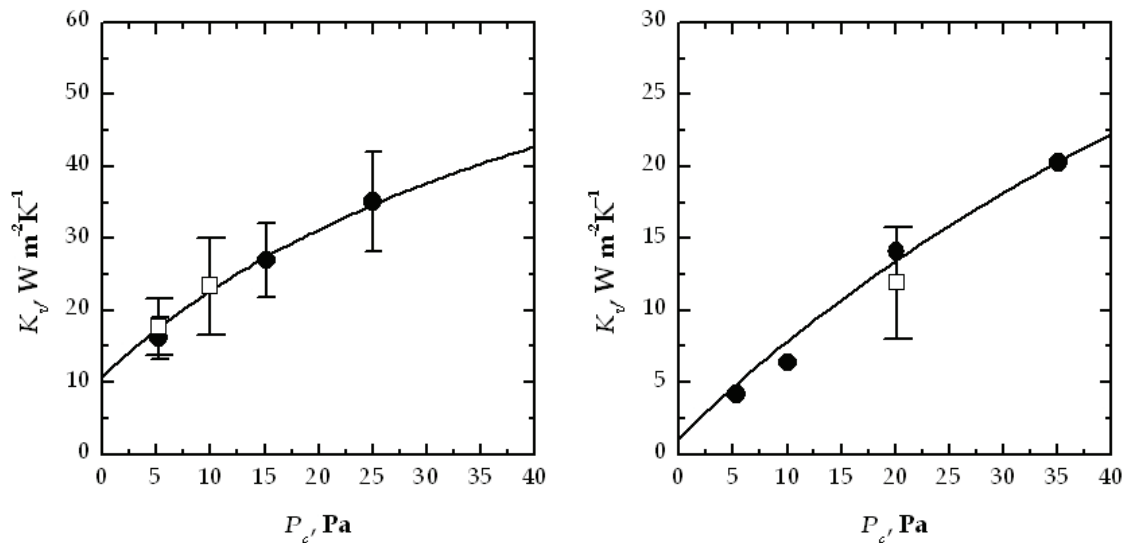


Fig. 3. Effect of chamber pressure on the value of K_v for the vial V₁ (left-side graph) and a stainless steel tray (right-side graph) processed in the laboratory freeze-dryer. The values calculated using the theoretical model, and the parameters of Table 3, are also displayed (solid line) together with the value estimated by pressure rise test technique (□)

In addition, it must be noticed that there is a large variance of K_v , which cannot be explained by the only observational error in the experiment, but is related to the heterogeneity of the lot. This is confirmed by the contour plot of Figure 4, where it can be observed that, because of side radiation and heat conduction though the metal frame, vials at the edge of the batch

have a higher value of K_v than those placed in the core. In particular, as already observed by Pisano at al. (2008), these additional contributions increase only the sublimation rate of vials placed just next to the additional heat sources, while their effect is reduced after the first row. However, this issue will be better discussed in the following section.

container	subset	C_1	C_2	C_3	σ_{C_1}
vials V_1	all the lot	10.9	1.4	0.04	4.9
vials V_1	B	21.9	1.4	0.04	6.3
vials V_1	C	13.6	1.4	0.04	1.5
vials V_1	D	9.7	1.4	0.04	0.5
vials V_1	E	7.8	1.4	0.04	0.1
metal tray	-	1.1	0.7	0.01	-

Table 3. Parameters required to calculate the value of K_v' vs. P_c for a metal tray (made of stainless steel) and the various groups of vials V_1

Let’s now focus on the temperature influence (of the gas trapped in the gap at the container bottom) on the value of K_v . In this study, as the gas temperature reasonably varies from the product temperature at the interface and T_{fluid} , it can be approximated to their mean. Figure 5 compares the heat transfer coefficient as measured at two different temperatures of the heating fluid, and thus of the chamber gas temperature, while the pressure inside the drying chamber is kept constant. It can be observed that a significant variation in the fluid temperature produces a modification of K_v that is of the same order of magnitude of the parameter uncertainty. This confirms that the dependence on gas temperature of K_v is not significant or, however, is very limited compared with the role of chamber pressure in the heat transfer.

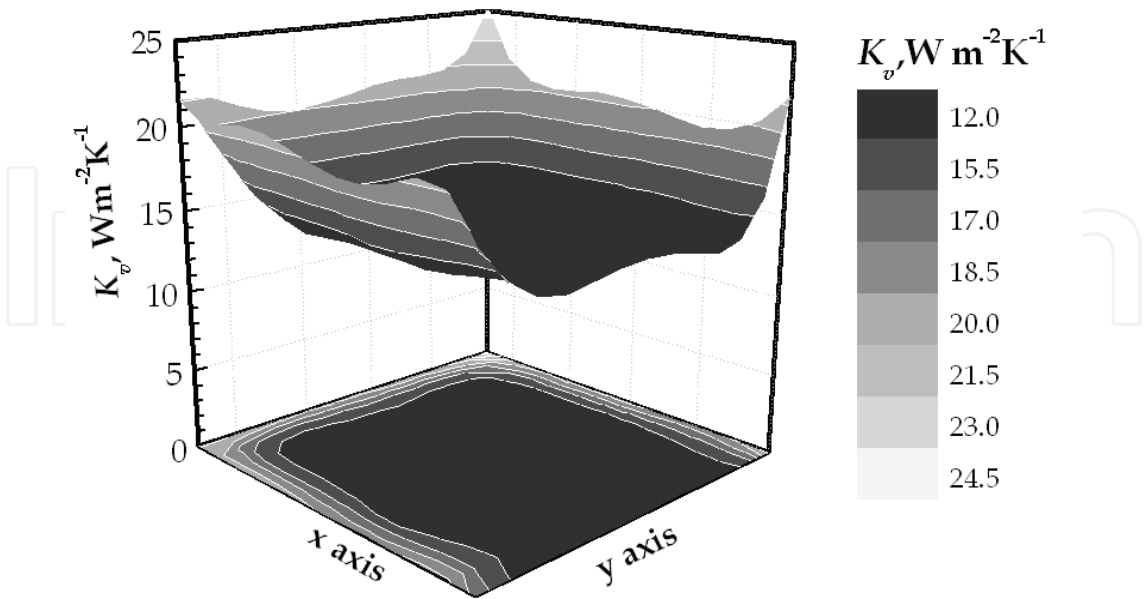


Fig. 4. Contour plot of the heat transfer coefficient for vials V_1 (loaded directly over the heating shelf) as measured over a lot. The primary drying phase was run at T_{fluid} =263 K and P_c =5 Pa. Results refer to a half of the batch

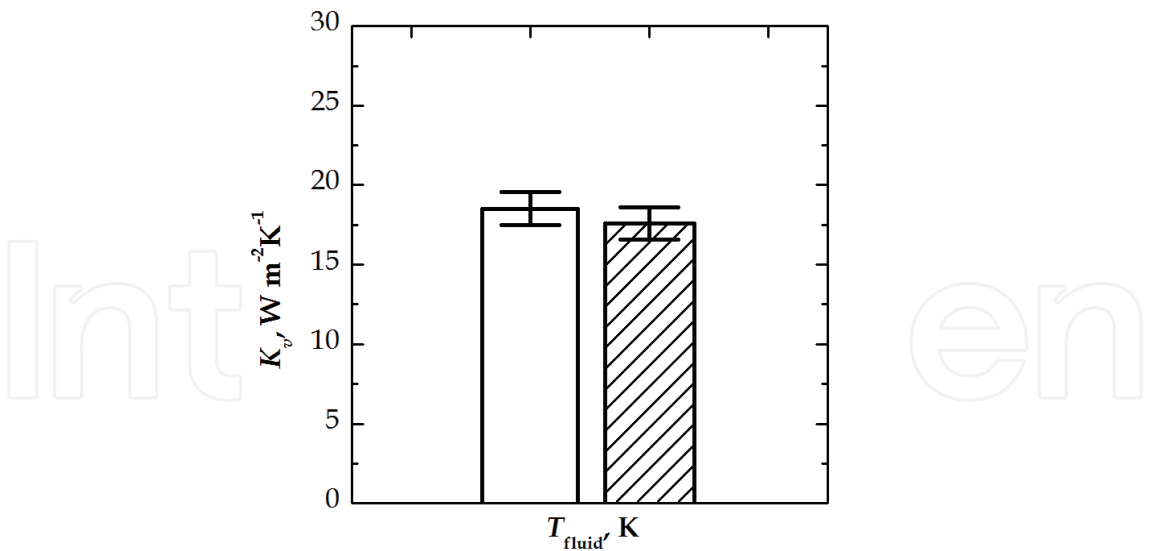


Fig. 5. Effect of T_{fluid} , and in turn of chamber gas temperature, on the value of K_v for the vial V_2 processed in the laboratory freeze-dryer. Both measurements were carried out at $P_c=10$ Pa, while the fluid temperature was set to: (□) $T_{\text{fluid}}=275$ K; (▨) $T_{\text{fluid}}=253$ K

Figure 3 (right-side graph) displays the value of K_v vs. P_c in case the process is carried out in trays. It can be observed that, similarly to what has been already shown for vials V_1 , the heat transfer coefficient is strongly influenced by the total chamber pressure. However, the value of K_v for trays is significantly lower than that of vials. This is probably due a bad contact between the tray bottom and the heating plate, as the resistance to heat transfer of the stainless steel tray is negligible. In addition, as already observed by Bruttini et al. (1991) for bulk freeze-drying of a solution of cloxacillin monosodium salt, it is confirmed that, for freeze-drying in trays, the heat is mostly transferred by the conduction through the thin layer of gas that separates shelf and tray surfaces.

In case of bulk freeze-drying, wherein the solution is poured in a metal tray, the heat transfer between the heating fluid and the product can be still calculated as the sum of the three terms of Equation (3). Therefore, the same mathematical model used for vials freeze-drying is here used to determine (via non-linear regression of experimental data) the optimal combination of a_c , K_c and ℓ that describes the pressure dependence of K_v for trays. The results so obtained are reported in Table 3.

4.2 Non uniformity of the lot

In the previous section it has been observed that the value of K_v significantly varies with the position of the vial in the lot, see Figure 4. Therefore, following on from what stated in section §3 (see Figure 1), the lot of vials has been divided in five zones, which are characterized by different heat transfer mechanisms. The criteria chosen to identify the various zones are summarized in Table 1.

As previously discussed, a further refinement might be introduced to distinguish vials radiated by different walls of the chamber, but it has not been considered here: the correctness of this approach is confirmed by the more detailed statistical analysis that is presented in the following.

Figure 6 compares the value of K_v vs. P_c for the various groups of vials identified in Table 1. Vials A were not considered in the analysis as only four samples can be monitored in each

test and, hence, the results are not statistically relevant. As it can be expected, the heat transfer coefficient of edge-vials (i.e. vials B and C) is much higher than that of vials placed in the core of the lot (i.e. vials D and E). In fact, according to Table 1, these vials receive an additional contribution of heat due to radiant energy coming from chamber walls and tray band, as well as, in case of vials B, the contribution due to conduction along the tray band.

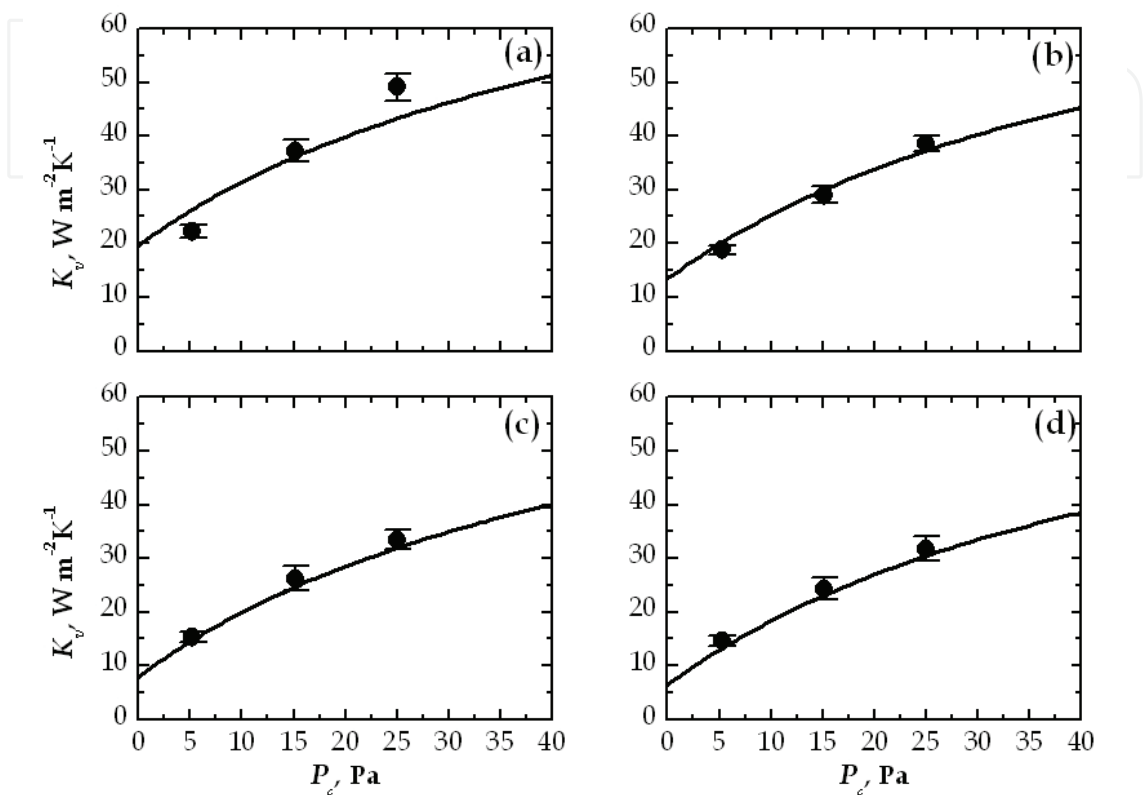


Fig. 6. Values of K_v vs. P_c for the four groups of vials (type V_1) identified in Table 1: (a) vials B; (b) vials C; (c) vials D and (d) E

Now let's focus on vials E, which are placed in the central part of the lot and, thus, are far from the edges where the contribution of the radiant heat from chamber walls can be relevant. Following on from what shown in section 2, the three parameters a_c , K_c and ℓ of vials V_1 , type E, can be obtained by a non-linear regression analysis of experimental data (Figure 6, graph d) that describes the pressure dependence of K_v . To obtain the model parameters of the other three groups of vials, we assume that a_c and ℓ , and thus C_2 and C_3 , are known, and equal to those determined for vials E. This assumption is reasonable, since these parameters depend on the container and not on the surrounding environment. On the contrary, K_c , and thus C_1 , is optimized to get the best fitting between model predictions and experimental observations. Table 3 summarizes the value of global parameters C_1 , C_2 and C_3 for the four groups of vials (V_1 type).

Concerning the uncertainty on the parameter K_v , it must be said that a_c and ℓ , thus C_2 and C_3 that define the pressure dependence of K_v , can be estimated, even if with some difficulties. On the contrary, it is almost impossible to estimate C_1 as it is affected by the contact between the shelf surface and the bottom of the container, as well as the view factors for the radiative heat. Furthermore, the effect on the final value of K_v due to the uncertainty on C_2 and C_3 (e.g. deriving from a different geometry of the container bottom) is less important than that due

to the variability associated to transport phenomena involved in C_1 . For all these reasons, we assume that the only responsible for the uncertainty on K_v is the parameter C_1 . Nevertheless, it is worth noticing that the uncertainty, or variability, on a_c and ℓ (and thus on C_2 and C_3) is implicitly included in the uncertainty on the parameter C_1 , even if it is not directly expressed. At this point, once the value of C_2 and C_3 is known, eq. (7) can be used for retrieving the coefficient C_1 of each vial of the lot (under investigation) from the value of K_v that has been previously measured for vials V_1 . Figure 7 displays the distribution of C_1 (of vials V_1) for the entire lot (graph a), as well as for the various families of vials of Table 1 (graphs b–e). It can be observed that the various groups of vials are characterized by a significantly different mean value of C_1 and, as it can be expected, edge-vials have a much higher C_1 than that of vials placed in the core of the batch.

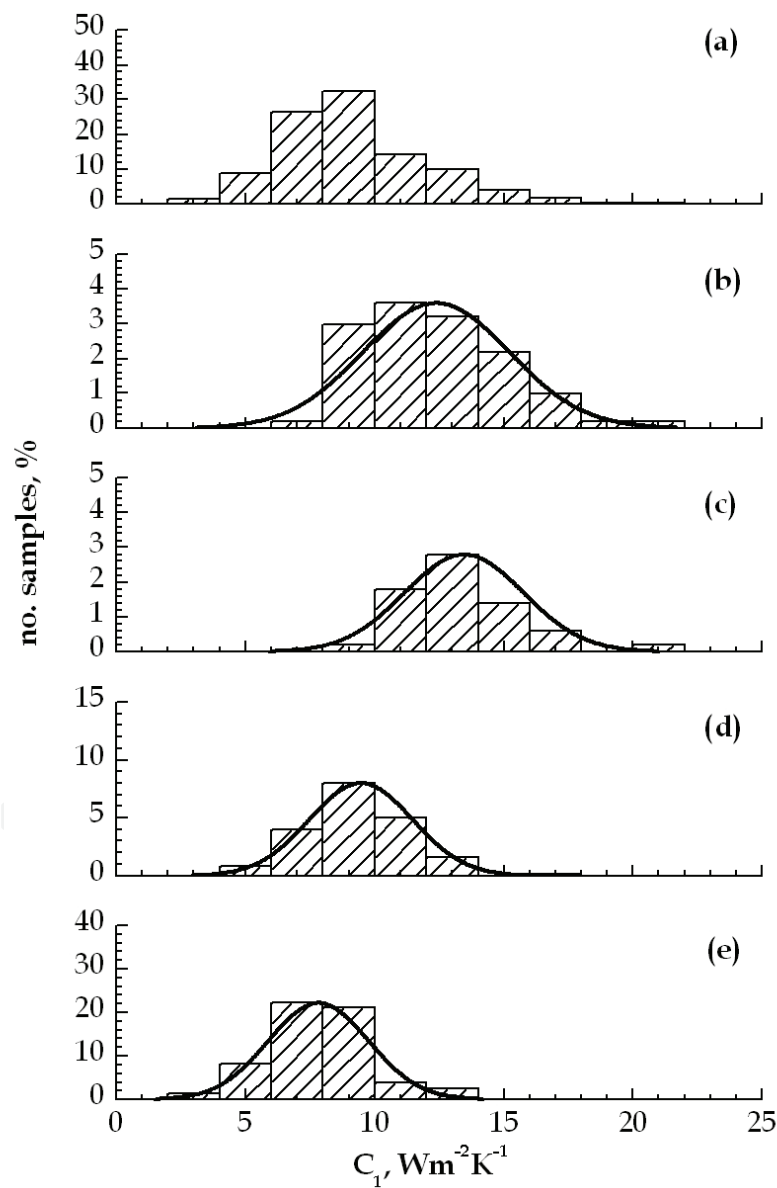


Fig. 7. Distribution of C_1 of vials V_1 for: (a) the entire lot; (b) vials B; (c) vials C; (d) vials D and (e) vials E. The solid line is the Gaussian distribution calculated according to the mean value and standard deviation reported in Table 3

In Figure 7 (graph a), the width of the C_1 distribution for the entire lot is so high that cannot be explained by the only observational error in the experiments but, as already discussed above, is due to the lot unevenness. Thus, the set of data has been divided in the four subsets previously identified and the distribution curve has been recalculated for each group of vials (see graphs b–e). The correctness of this approach is confirmed by the fact that the resulting curves can be well described by Gaussian distributions (that are typically used for describing the observational error in an experiment) and their width is significantly reduced. It can be noticed that the variance of C_1 for vials B is still relevant (even if much smaller than that of the entire lot), but it is now difficult to discern the contribution due to the intrinsic variability of the object of measurement from the uncertainty of the method.

4.3 Role of the vials geometry and material

Following on from what stated in section §2, the shape of the container bottom significantly affects the value of K_v , as well as its dependence on chamber pressure. To better investigate this aspect, the heat transfer coefficient of two different types of vials (i.e. V_1 and V_2), which have a similar geometry (in terms of external diameter and side-wall thickness), but a different shape of the bottom, are compared.

The values of K_v vs. P_c for the two types of containers, and in case they are directly loaded on the heating shelf and processed in the same equipment, are displayed in Figure 8. To discern the contributions due to the characteristics of the vial from those of the environment, the analysis is limited to only those vials that are placed in the centre of the lot. It can be noticed that the two containers have a similar value of C_1 even if vials V_2 have a thicker vial bottom wall.

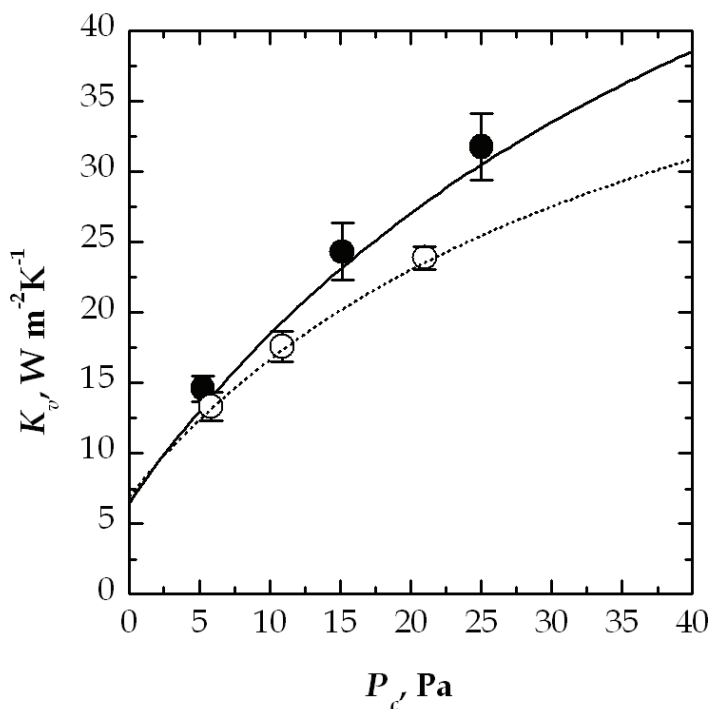


Fig. 8. Comparison between the value of K_v vs. P_c for vials subset E (processed in the laboratory freeze-dryer) in case of two different container geometries: (●) V_1 and (○) V_2 type. The values calculated using the theoretical model are also displayed: (solid line) vials V_1 and (dotted line) V_2

In particular, as the containers have a similar geometry and the contact between the container bottom and the shelf plate tightly depends on the characteristics of the vial surface, this implies that, in this case, the heat conduction (at the points of contact between the container bottom and the shelf surface) and the radiative heat coming from the heating plate give a similar contribution to the energy balance.

On the contrary, it can be observed a significantly different pressure dependence of K_v . This is due to a different contribution of the heat conduction through the gas trapped at the container bottom to the total energy balance of the vial. According to manufacturer specifications, the maximum value of the gap thickness is greater in vials V_1 ($\ell_{\max}=4.0\times10^{-4}$ m) and this seems to be in disagreement with experimental results of Figure 8. Nevertheless, it must be said that the heat conduction through the gas is a function of the volume of the gas gap, which depends not only on ℓ_{\max} , but also on the shape of the vial bottom. In particular, the visual inspection of the two systems confirms that vials V_1 , despite a higher value of ℓ_{\max} , are characterized by a flatter gap at the bottom. As a consequence, the heat transfer resistance due to the gas gap is lower in vials V_1 , which show a marked pressure dependence of K_v . As further confirmation of the previous evidences, the effective value of ℓ , as obtained by a non-linear regression of experimental data, of vials V_1 ($\ell=2.0\times10^{-4}$ m) is smaller than that of vials V_2 ($\ell=3.1\times10^{-4}$ m).

A final comment concerns the effect of container treatments (e.g. a silane coating of the internal vial walls) on the value of K_v . Figure 9 compares the overall heat transfer coefficient of vials V_2 in case they underwent a silane coating treatment or not. It can be noticed that pre-treated vials show a lower value of K_v and this reduction is of the same order of magnitude for all the four group of vials, thus the coating does not alter the contribution of the radiative heat to the total energy balance of the vial, but probably only the conduction through the vial side-wall.

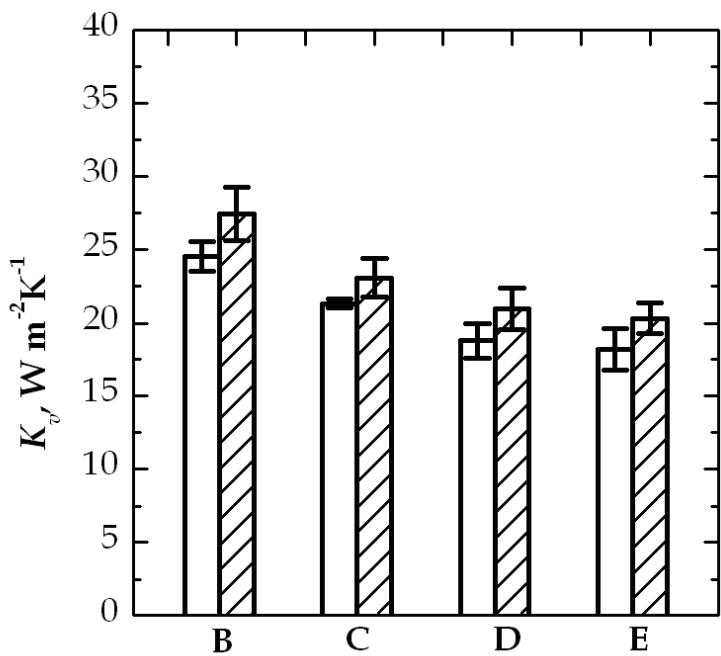


Fig. 9. Heat transfer coefficient of the four groups of vials (V_2 type) in case they underwent a silane coating treatment (void bars) or not (filled bar). The lot of vials is loaded on the heating shelf and enclosed by an external metal band. The measurement was carried out at $P_c=10$ Pa

4.4 Role of the configuration used for containers loading

In this section, we compare the value of K_v , as well as the heterogeneity of the lot, in case various configurations are used for loading the product into the drying chamber; in particular, the following configurations have been investigated:

- Vials are directly loaded on the heating shelf and enclosed by a metal frame;
- Vials are directly loaded on the heating shelf, but not surrounded by a frame;
- Vials are loaded on a metal tray.

Figure 10 compares the heat transfer coefficient of vials in case they are enclosed by a metal frame or not (the comparison is carried out for vials V_2). In particular, the use of a metal frame can have a different effect on the heat transfer coefficient of the various groups of vials. For example, the mean value of K_v for vials E is not significantly modified by the presence of the surrounding band, while edge-vials (both vials B and C) show a much higher value of K_v in case no metal frame is used. In fact, this frame acts as thermal shield since it reduces the radiative heat coming from chamber walls, which are warmer than the metal frame. The metal band also minimizes the unevenness of edge vials, as they are not anymore exposed to surfaces with different characteristics and temperature. Nevertheless, it must be said that edge-vials continue to receive an additional heat flow (due to the conduction between the vial side-wall and the metal band at the points of contact), but this has a minor effect with respect to chamber walls radiation. All these effects tightly depend upon the type of frame used, as well as the geometry of the drying chamber; hence, it is fundamental to take into account such phenomena during process transfer from one unit to another one, mainly if the loading configuration is modified.

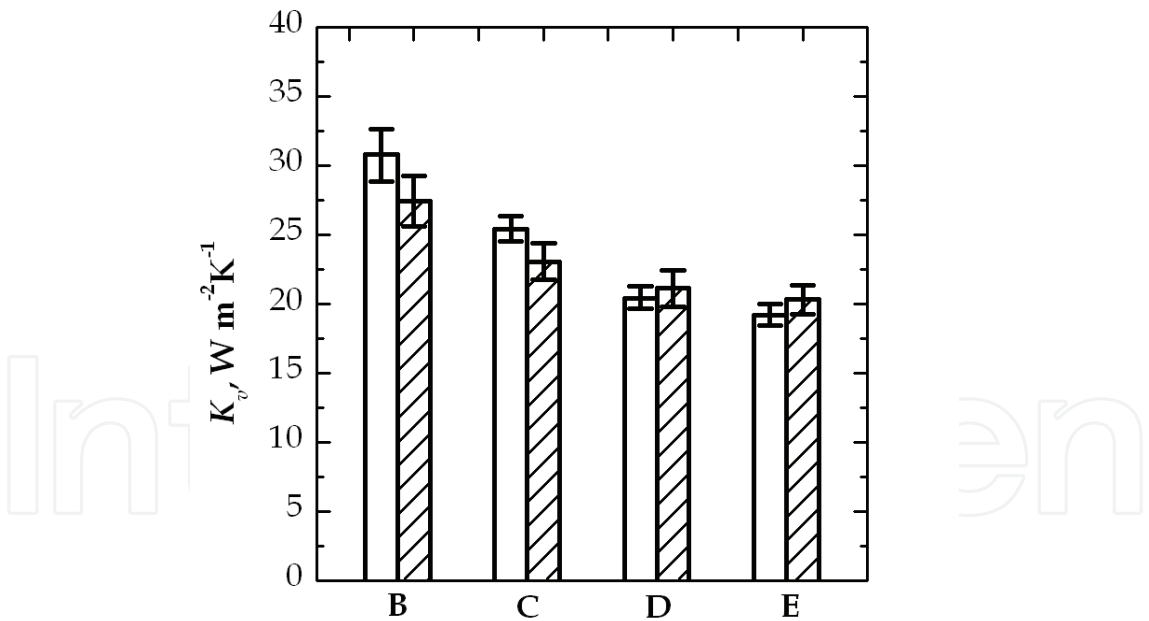


Fig. 10. Heat transfer coefficient (at $P_c=10$ Pa) of the four groups of vials (V_2 type, silane treated) in case of two different loading configurations: (void bars) the lot of vials is loaded on the heating shelf; (filled bar) the lot of vials is loaded on the heating shelf and enclosed by an external metal band

Figure 11, instead, compares the value of K_v in case vials are loaded on a metal tray or directly loaded on the heating shelf; the comparison was carried out for vials V_3 . It can be noticed that if on one side the use of a tray introduces an additional resistance to the heat

transfer, on the other side it allows to get a more uniform distribution of the heat over the lot (in Figure 11, the error bar is much smaller in case vials are loaded on a tray), as well as a strong reduction of the value of K_v for edge-vials due to the presence of the tray band. This strongly reduces the difference of K_v between vials D and E, as those vials that are located on the second row of the lot are now in contact with vials that are less warm and, thus, receive a smaller amount of heat from edge-vials.

Figure 12 (a) compares the value of K_v for vials loaded on the heating plate or in trays made of different materials, i.e. stainless steel or polystyrene. Even in this case we can observe a strong reduction of K_v when vials are loaded on a tray. In particular, the value of K_v of central vials (both group D and E) is not modified by the type of tray used; in fact, the observed variations are of the same order of magnitude of the error bar. On the contrary, K_v of edge-vials significantly changes with the type of tray used. This can be explained by a different heat transfer between the tray band and the container side-walls, which, for example, can be due to a different emissivity of the tray material.

4.5 Role of the equipment size

Figure 12 (b) compares the heat transfer coefficient of vials processed in laboratory and manufacturing equipment. Results refer to vials loaded on a plastic tray and in case the drying is carried out at $P_c=10$ Pa. It can be observed that the value of K_v of vials located in the central part of the lot is not significantly modified, whereas edge-vials processed in the laboratory freeze-dryer have a higher value of K_v than that observed in the large scale freeze-dryer. This is due to a different contribution of the radiative heat (that, for example, can be caused by a different geometry of the drying chamber) and has to be taken into account when we have to transfer a process from one unit to another one, as well as during scale-up operations, as the fraction of edge-vials into the lot varies with the scale of the equipment.

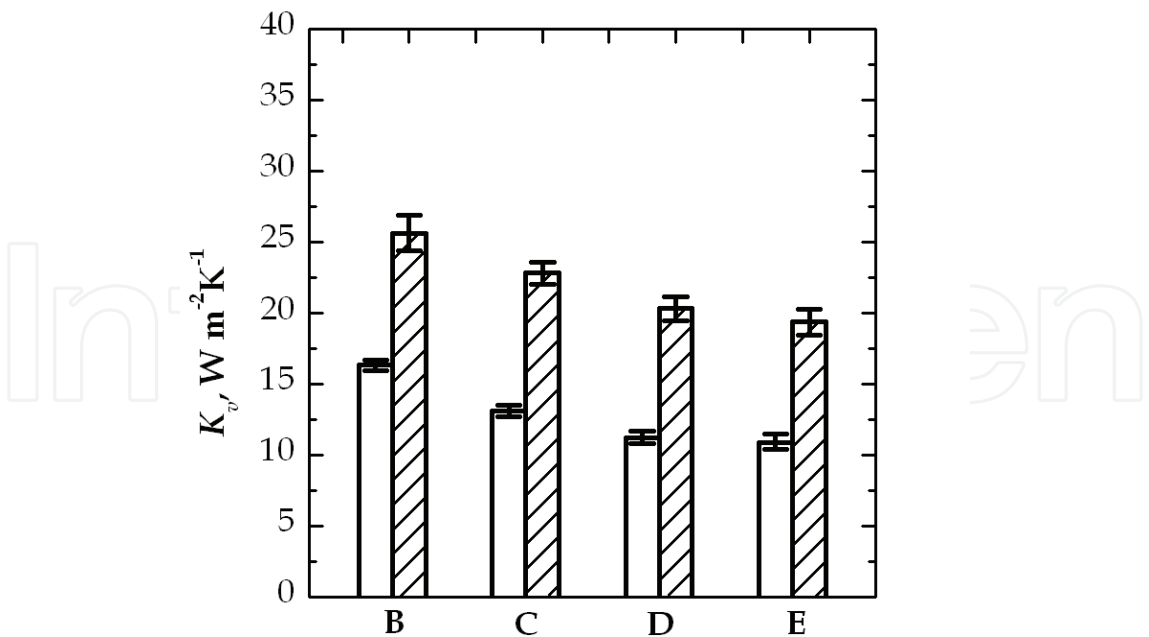


Fig. 11. Heat transfer coefficient (at $P_c=10$ Pa) of the four groups of vials (V_3 type) in case of two different loading configurations: (void bars) the lot of vials is loaded on a metal tray; (filled bar) the lot of vials is loaded on the heating shelf and enclosed by an external metal band

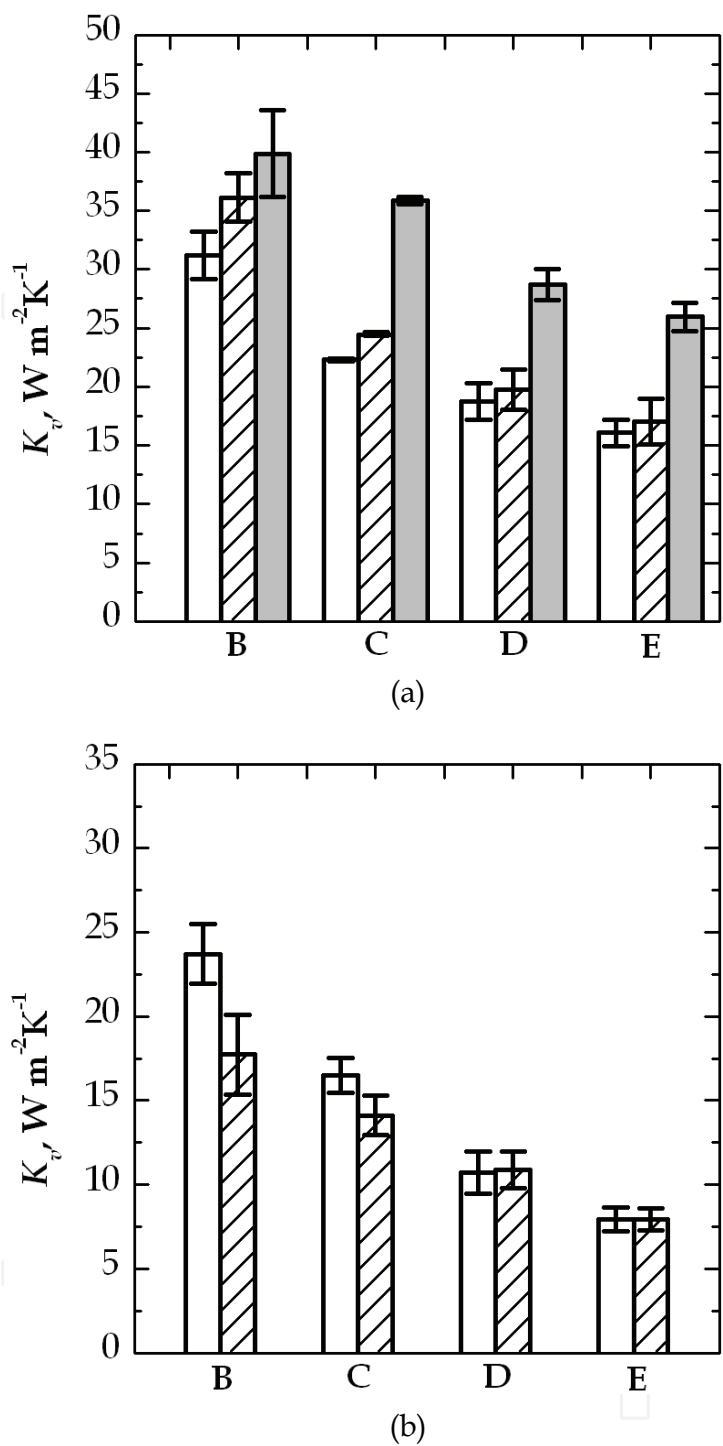


Fig. 12. Comparison between experimental values of K_v for the various groups of vials (V_4 type). (a) Influence of various loading configurations: vials loaded on a stainless steel tray (\square), a polystyrene tray (hatched) and directly on the heating shelf (grey); (b) values measured in two pieces of equipment of different size: (\square) laboratory and (hatched) industrial scale dryer

For the two pieces of equipment investigated in this study, central vials have almost the same value of K_v , but, in general, it can happen to observe significant differences. In fact, even if the value of ℓ is independent of the equipment used, the parameters a_c and K_c can be affected by the characteristics of the shelf surface. Thus, once the value of ℓ has been

determined for the laboratory freeze-dryer (using the procedure described in section §2), and assuming that a_c does not change, we can calculate the effective value of K_c for the four groups of vials in case they are processed in the industrial freeze-dryer. It follows that the global coefficients C_2 and C_3 , which describe the pressure dependence of K_v , are the same for both pieces of equipment, while the parameter C_1 of peripheral vials is slightly different (as it depends on the vial-tray and shelf-tray contact, and on radiation effect). The knowledge of the pressure dependence of K_v in the two pieces of equipment is fundamental to make decisions during the phase of scale-up of a recipe obtained in a laboratory scale equipment to an industrial scale freeze-dryer.

5. Conclusion

Following on from what stated in the introduction, the heat transfer to the product has to be carefully controlled in order to avoid product overheating. This result can be obtained in-line, using a control system (Pisano et al., 2010, 2011), or building off-line the design space, i.e. identifying the set of operating conditions (heating fluid temperature and chamber pressure) that allows preserving product quality. Recently, the use of mathematical modelling, coupled with few experiments to determine model parameters (e.g. the value of K_v vs. P_c), has been proposed to get the design space quickly, taking also into account the effect of parameters uncertainty and/or variability (Giordano et al., 2011).

Due to batch non-uniformity, vials have to be divided in various subsets (as shown above), which are characterized by the same value of K_v , and the design space (that is strongly dependent on the value of K_v) has to be built for each group (Fissore et al., 2011b). Of course, since the design space of edge-vials is more contracted than that of vials placed in the core, processing conditions has to be chosen according to the design space of those vials that can be more easily damaged by product overheating (i.e. vials B). The recipe so designed allows preserving product quality of the entire lot, but the resulting drying time might be quite long. Therefore, as edge-vials are a small fraction of the lot, it might be worth referring to central vials to reduce the duration of the process. Of course, this is advantageous only if the energy saving deriving from a shorter drying time compensate the loss due to product waste (that derives from the fact that edge vials did not meet product quality criteria).

It must be remarked that whichever is the tool used to control the process, the resulting recipe is strongly dependent on the value of K_v , which can vary with operating conditions, type of container, equipment and configuration used for loading the product.

The experimental investigation carried out in this study has evidenced a strong dependence of the heat transfer coefficient on processing conditions used for the drying. In particular, it has been proved that while the gas temperature has a minor effect on the value of K_v , the role of chamber pressure cannot be neglected. To be used by the model at the basis of the various tools recently developed for the recipe design, the pressure dependence of K_v has been described by a mathematical model, whose parameters have been obtained, for various types of container (both glass vials and trays), by regression analysis of experimental data.

In addition, the heat transfer of glass vials has been measured in case of various loading configurations. It has been shown that, as expected, the introduction of a tray significantly reduces the value of the heat transfer coefficient of the entire lot and, in particular, a more marked reduction was observed for edge-vials. On the contrary, in case vials are directly loaded on the shelf, but surrounded by a metal frame, the value of K_v of central vials is not

modified, while that of edge vials is strongly reduced. This is due to the contribution of the tray band, which acts as thermal shield for the radiative heat coming from chamber walls. Therefore, it must be remarked that, during the phase of process development, the user has to take into account that the pressure dependence of K_v does not depend only on the type of vials, but also on the configuration used for loading the product into the drying chamber.

In general, the gravimetric procedure gives the best accuracy and robustness, even if it is more time demanding with respect to other global methods available. However, the use of the pressure rise test technique is strongly suggested in case of industrial apparatus, where the gravimetric procedure is not practicable as the intervention of the user (to place temperature sensors over the lot of vials) is limited. Therefore, it has been shown that the pressure rise test technique (and in particular the latest developments like the DPE⁺ algorithm) can be effectively used for measuring the value of K_v , whichever is the scale of the equipment, without requiring an excessive effort from the users. In addition, an estimation of the mean value of K_v is more than enough for an effective description of the heat transfer of the lot, as the effect of batch non-uniformity in a manufacturing process is less marked. A further advantage of the pressure rise test technique is that, with respect to other global methods like TDLAS, it requires no modifications of the equipment and its hardware.

A final comment concerns the problem of scale-up, or process transfer, of a recipe from one unit to another one. It has been proved that the heat transfer coefficient of a specific container can varies significantly (mainly for edge vials) with the type of equipment used, even if the same loading configuration is used. Therefore, if this difference is relevant, the recipe, which is usually developed in laboratory and has to be transferred on manufacturing equipment, should be adapted to take into account the different heat transfer of the containers.

6. Acknowledgment

Development of PRT methods for industrial apparatus has been continuously supported by Telstar S.A. (Terrassa, Spain), whose contribution of data obtained in large scale apparatus and financial support for this chapter is gratefully acknowledged. The authors would like to acknowledge Giovanni Accardo, Salvatore Genco e Daniele Sorce for their valuable support in the experimental investigation.

7. Nomenclature

a_c	energy accommodation coefficient
A_v	cross sectional area of the vial, m ²
A_{sub}	total sublimation area, m ²
C_1	parameter expressing the dependence of K_v' from radiation and the contact between vial bottom and tray surface, J s ⁻¹ m ⁻² K ⁻¹
C_2	parameter expressing the pressure dependence of K_v' , J s ⁻¹ m ⁻² K ⁻¹ Pa ⁻¹
C_3	parameter expressing the pressure dependence of K_v , Pa ⁻¹
e_s	emissivity for radiation heat exchange from the shelf to the bottom of the vial
e_v	emissivity for radiation heat exchange from the shelf to the top of the vial
ΔH_s	heat of sublimation, J kg ⁻¹
J_q	heat flux to the product, J s ⁻¹ m ⁻²
J_w	solvent flux, kg s ⁻¹ m ⁻²

k_s	heat transfer coefficient between the technical fluid and the shelf, $\text{J s}^{-1}\text{m}^{-2}\text{K}^{-1}$
K_c	heat transfer coefficient due to direct conduction from the shelf to the glass at the points of contact, $\text{J s}^{-1}\text{m}^{-2}\text{K}^{-1}$
K_g	heat transfer coefficient due to conduction in the gas between the shelf and the vial bottom, $\text{J s}^{-1}\text{m}^{-2}\text{K}^{-1}$
K_r	heat transfer coefficient between the shelf and the vial due to radiation, $\text{J s}^{-1}\text{m}^{-2}\text{K}^{-1}$
K_v	overall heat transfer coefficient between the heating fluid and the product at the bottom of the vial, $\text{J s}^{-1}\text{m}^{-2}\text{K}^{-1}$
K'_v	overall heat transfer coefficient between the heating shelf and the vial bottom (or between shelf and tray, and tray and vials), $\text{J s}^{-1}\text{m}^{-2}\text{K}^{-1}$
K_v^*	overall heat transfer coefficient between the heating shelf and the product at the bottom of the vial, $\text{J s}^{-1}\text{m}^{-2}\text{K}^{-1}$
ℓ	constant effective distance between the bottom of the vial and the shelf, m
m	mass, kg
M_w	molar mass of water, kg kmol^{-1}
$p_{w,c}$	partial pressure of water in the drying chamber, Pa
P_c	chamber pressure, Pa
R	ideal gas constant, $\text{J kmol}^{-1}\text{K}^{-1}$
s_g	thickness of the glass at the bottom of the vial, m
s_{tray}	thickness of the tray bottom, m
t	time, s
T	temperature, K
T_B	temperature of the product at the vial bottom, K
T_c	temperature of the chamber gas, K
T_{fluid}	temperature of the heating fluid, K
T_{shelf}	temperature of the heating shelf, K
V_c	volume of the drying chamber, m^3
<i>Greeks</i>	
α	parameter used to calculate K_g
κ	Stefan-Boltzman constant, $\text{J s}^{-1}\text{m}^{-2}\text{K}^{-4}$
Λ_0	free molecular heat conductivity at 0°C , $\text{J s}^{-1}\text{m}^{-1}\text{K}^{-1}$
λ_0	heat conductivity of the water vapour at ambient pressure, $\text{J s}^{-1}\text{m}^{-1}\text{K}^{-1}$
λ_g	heat conductivity of the glass, $\text{J s}^{-1}\text{m}^{-1}\text{K}^{-1}$
λ_{tray}	heat conductivity of the tray, $\text{J s}^{-1}\text{m}^{-1}\text{K}^{-1}$
σ_{C_1}	standard deviation of the parameter C_1 , $\text{J s}^{-1}\text{m}^{-2}\text{K}^{-1}$

8. References

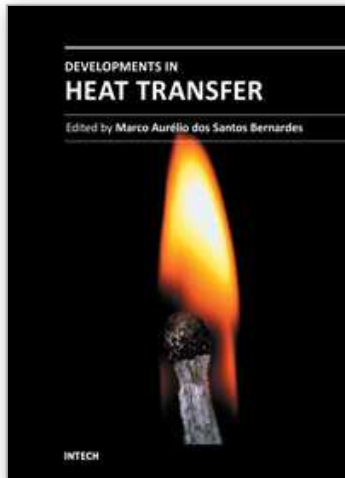
- Brülls, M., & Rasmuson, A. (2002). Heat transfer in vial lyophilization. *International Journal of Pharmaceutics*, Vol. 246, pp. 1-16, ISSN 0378-5173.
- Bruttini, R., Rovero, G., & Baldi, G. (1991). Experimentation and modelling of pharmaceutical lyophilization using a pilot plant. *The Chemical Engineering Journal*, Vol. 45, pp. B67-77, ISSN 1385-8947.
- Chen, R., Slater, N. K. H., Gatlin, L. A., Kramer, T., & Shalaev, E. Y. (2008). Comparative rates of freeze-drying for lactose and sucrose solutions as measured by

- photographic recording, product temperature and heat flux transducer. *Pharmaceutical Development and Technology*, Vol. 13, pp. 367-374, ISSN 1083-7450.
- Chouvenc, P., Vessot, S., Andrieu, J., & Vacus P. (2004). Optimization of the freeze-drying cycle: a new model for pressure rise analysis. *Drying Technology*, Vol. 22, pp. 1577-1601, ISSN 1532-2300.
- Corbellini, S., Parvis, M., & Vallan, A (2010). In-process temperature mapping system for industrial freeze dryers. *IEEE Transactions on Instrumentation and Measurement*, Vol. 59, pp. 1134-1140, ISSN 0018-9456.
- Dushman, S., & Lafferty, J. M. (1962). *Scientific foundations of vacuum technique*, Wiley, ISBN 978-047-1228-03-5, New York, USA.
- Fissore, D., Pisano, R., & Barresi, A. A. (2011a). On the methods based on the Pressure Rise Test for monitoring a freeze-drying process. *Drying Technology*, Vol. 29, pp. 73-90, ISSN 1532-2300.
- Fissore, D., Pisano, R., & Barresi, A. A. (2011b). Advanced approach to build the design space for the primary drying of a pharmaceutical freeze-drying process. Submitted to *Journal of Pharmaceutical Sciences*, ISSN 0022-3549.
- Franks, F. (2007). *Freeze-drying of pharmaceuticals and biopharmaceuticals*, Royal Society of Chemistry, ISBN 978-085-4042-68-5, Cambridge, UK.
- Gan, K. H., Bruttini, R., Crosser, O. K., & Liapis, A. A. (2005a). Freeze-drying of pharmaceuticals in vials on trays: effects of drying chamber wall temperature and tray side on lyophilization performance. *International Journal of Heat and Mass Transfer*, Vol. 48, pp. 1675-1687, ISSN 0017-9310.
- Gan, K. H., Crosser, O. K., Liapis, A. I., & Bruttini, R. (2005b). Lyophilisation in vials on trays: effects of tray side. *Drying Technology*, Vol. 23, pp. 341-363, ISSN 1532-2300.
- Gieseler, H., Kessler, W. J., Finson, M., Davis, S. J., Mulhall, P. A., Bons, V., Debo, D. J., & Pikal, M. J. (2007). Evaluation of Tunable Diode Laser Absorption Spectroscopy for in-process water vapor mass flux measurement during freeze drying. *Journal of Pharmaceutical Sciences*, Vol. 96, pp. 1776-1793, ISSN 0022-3549.
- Giordano, A., Barresi, A. A., & Fissore, D. (2011). On the use of mathematical models to build the design space for the primary drying phase of a pharmaceutical lyophilization process. *Journal of Pharmaceutical Sciences*, Vol. 100, pp. 311-324, ISSN 0022-3549.
- Hottot, A., Vessot, S., & Andrieu, J. (2005). Determination of mass and heat transfer parameters during freeze-drying cycles of pharmaceutical products. *PDA Journal of Pharmaceutical Science and Technology*, Vol. 59, pp. 138-53, ISSN 1079-7440.
- Jennings, T. A. (1999) *Lyophilization: introduction and basic principles*, CRC Press, ISBN 978-157-4910-81-0, Boca Raton, USA.
- Kessler, W. J., Davis, S. J., Mulhall, P. A., & Finson, M. L. (2006). System for monitoring a drying process. United States Patent No. 0208191 A1.
- Kuu, W. Y., Nail, S. L., & Sacha, G. (2009). Rapid determination of vial heat transfer parameters using tunable diode laser absorption spectroscopy (TDLAS) in response to step-changes in pressure set-point during freeze-drying. *Journal of Pharmaceutical Sciences*, Vol. 98, pp. 1136-1154, ISSN 0022-3549.
- Mellor, J. D. (1978). *Fundamentals of freeze-drying*, Academic Press, ISBN 978-012-4900-50-9, London, UK.

- Milton, N., Pikal, M. J., Roy, M. L., & Nail, S. L. (1997). Evaluation of manometric temperature measurement as a method of monitoring product temperature during lyophilisation. *PDA Journal of Pharmaceutical Science and Technology*, Vol. 5, pp. 7-16, ISSN 1079-7440.
- Oetjen, G. W., & Haseley, P. (2004). *Freeze-Drying*, Wiely-VHC, ISBN 978-352-7306-20-6, Weinheim, Germany.
- Pikal, M. J. (1985). Use of laboratory data in freeze-drying process design: heat and mass transfer coefficients and the computer simulation of freeze-drying. *Journal of Parenteral Science and Technology*, Vol. 39, pp. 115-139, ISSN 0279-7976.
- Pikal, M. J. (2000). Heat and mass transfer in low pressure gases: applications to freeze-drying. In: *Transport processes in pharmaceutical systems*, Amidon, G. L., Lee, P. I., & Topp, E. M., pp. 611-686, Marcel Dekker, ISBN 0-8247-66105, New York, USA.
- Pikal, M. J., & Shah, S. (1990). The collapse temperature in freeze drying: dependence on measurement methodology and rate of water removal from the glassy phase, *International Journal of Pharmaceutics*, Vol. 62, pp. 165-186, ISSN 0378-5173.
- Pikal, M. J., Roy, M. L., & Shah, S. (1984). Mass and heat transfer in vial freeze-drying of pharmaceuticals: role of the vial. *Journal of Pharmaceutical Sciences*, Vol. 73, pp. 1224-1237, ISSN 0022-3549.
- Pisano, R., Fissore, D., & Barresi, A. A. (2011). Freeze-drying cycle optimization using Model Predictive Control techniques. *Industrial & Engineering Chemistry Research*, Vol. 50, pp. 7363-7379, ISSN 0888-5885.
- Pisano, R., Fissore, D., Velardi, S. A., & Barresi, A. A. (2010). In-line optimization and control of an industrial freeze-drying process for pharmaceuticals. *Journal of Pharmaceutical Sciences*, Vol. 99, pp. 4691-4709, ISSN 0022-3549.
- Pisano, R., Rasetto, V., Petitti, M., Barresi, A. A., & Vallan, A. (2008). Modelling and experimental investigation of radiation effects in a freeze-drying process, *Proceedings of EMMC- 5th Chemical Engineering Conference for Collaborative Research in Eastern Mediterranean Countries*, pp. 394-398, Cetraro (CS), Italy, May 24-29, 2008.
- Rambhatla, S., Obert, J. P., Luthra, S., Bhugra, C., & Pikal, M. J. (2005). Cake shrinkage during freeze drying: a combined experimental and theoretical study, *Pharmaceutical Development & Technology*, Vol. 1, pp. 33-40, ISSN 0265-2048.
- Rambhatla, S., & Pikal, M. J. (2003). Heat and mass transfer scale-up issues during freeze-drying, I: atypical radiation and edge vial effect. *AAPS PharmSciTech*, Vol. 4, Article No. 14, ISSN: 1530-9932.
- Sadikoglu, H., Ozdemir, M., & Seker, M. (2006). Freeze-drying of pharmaceutical products: research and development needs. *Drying Technology*, Vol. 24, pp. 849-861, ISSN 0737-3937.
- Schneid, S. & Gieseler, H. (2008). Evaluation of a new wireless temperature remote interrogation system (TEMPRIS) to measure product temperature during freeze-drying. *AAPS PharmSciTech*, Vol. 9, pp. 729-739, ISSN 1530-9932.
- Sheehan, P., & Liapis, A. I. (1998). Modeling of the primary and secondary drying stages of the freeze-drying of pharmaceutical product in vials: numerical results obtained from the solution of a dynamic and spatially multi-dimensional lyophilisation model for different operational policies. *Biotechnology & Bioengineering*, Vol. 60, pp. 712-728, ISSN 1097-0290.

- Tang, X. C., Nail, S. L., & Pikal, M. J. (2006). Evaluation of manometric temperature measurement (MTM), a process analytical technology tool in freeze-drying, part III: heat and mass transfer measurement. *AAPS PharmSciTech*, Vol. 7, Article No. 97, ISSN 1530-9932.
- Velardi, S. A., & Barresi, A. A. (2008). Development of simplified models for the freeze-drying process and investigation of the optimal operating conditions. *Chemical Engineering Research and Design*, Vol. 86, pp. 9-22, ISSN 0263-8762.
- Velardi, S. A., Rasetto, V., & Barresi A. A. (2008). Dynamic Parameters Estimation Method: advanced Manometric Temperature Measurement approach for freeze-drying monitoring of pharmaceutical solutions. *Industrial Engineering Chemistry Research*, Vol. 47, pp. 8445-8457, ISSN 0888-5885.
- Wang, W. (2000). Lyophilization and development of solid protein pharmaceuticals, *International Journal of Pharmaceutics*, Vol. 203, pp. 1-60, ISSN 0378-5173.

IntechOpen



Developments in Heat Transfer

Edited by Dr. Marco Aurelio Dos Santos Bernardes

ISBN 978-953-307-569-3

Hard cover, 688 pages

Publisher InTech

Published online 15, September, 2011

Published in print edition September, 2011

This book comprises heat transfer fundamental concepts and modes (specifically conduction, convection and radiation), bioheat, entransy theory development, micro heat transfer, high temperature applications, turbulent shear flows, mass transfer, heat pipes, design optimization, medical therapies, fiber-optics, heat transfer in surfactant solutions, landmine detection, heat exchangers, radiant floor, packed bed thermal storage systems, inverse space marching method, heat transfer in short slot ducts, freezing and drying mechanisms, variable property effects in heat transfer, heat transfer in electronics and process industries, fission-track thermochronology, combustion, heat transfer in liquid metal flows, human comfort in underground mining, heat transfer on electrical discharge machining and mixing convection. The experimental and theoretical investigations, assessment and enhancement techniques illustrated here aspire to be useful for many researchers, scientists, engineers and graduate students.

How to reference

In order to correctly reference this scholarly work, feel free to copy and paste the following:

Roberto Pisano, Davide Fissore and Antonello A. Barresi (2011). Heat Transfer in Freeze-Drying Apparatus, Developments in Heat Transfer, Dr. Marco Aurelio Dos Santos Bernardes (Ed.), ISBN: 978-953-307-569-3, InTech, Available from: <http://www.intechopen.com/books/developments-in-heat-transfer/heat-transfer-in-freeze-drying-apparatus>

INTECH
open science | open minds

InTech Europe

University Campus STeP Ri
Slavka Krautzeka 83/A
51000 Rijeka, Croatia
Phone: +385 (51) 770 447
Fax: +385 (51) 686 166
www.intechopen.com

InTech China

Unit 405, Office Block, Hotel Equatorial Shanghai
No.65, Yan An Road (West), Shanghai, 200040, China
中国上海市延安西路65号上海国际贵都大饭店办公楼405单元
Phone: +86-21-62489820
Fax: +86-21-62489821

© 2011 The Author(s). Licensee IntechOpen. This chapter is distributed under the terms of the [Creative Commons Attribution-NonCommercial-ShareAlike-3.0 License](https://creativecommons.org/licenses/by-nc-sa/3.0/), which permits use, distribution and reproduction for non-commercial purposes, provided the original is properly cited and derivative works building on this content are distributed under the same license.

IntechOpen

IntechOpen